

Supporting Information

for *Adv. Sci.*, DOI 10.1002/adv.202301939

The Lipid Metabolism as Target and Modulator of BOLD-100 Anticancer Activity: Crosstalk with Histone Acetylation

*Dina Baier, Theresa Mendrina, Beatrix Schoenhacker-Alte, Christine Pirker, Thomas Mohr, Mate Rusz, Benedict Regner, Martin Schaier, Nicolas Sgarioto, Noël J.-M. Raynal, Karin Nowikovsky, Wolfgang M. Schmidt, Petra Heffeter, Samuel M. Meier-Menches, Gunda Koellensperger, Bernhard K. Keppler and Walter Berger**

Supporting Information

The lipid metabolism as target and modulator of BOLD-100 anticancer activity: crosstalk with histone acetylation.

Dina Baier^{1,2,3}, Theresa Mendrina^{1,2,3}, Beatrix Schoenhacker-Alte^{1,2,3}, Christine Pirker^{1,3}, Thomas Mohr^{1,5,9}, Mate Rusz^{2,3,4}, Benedict Regner⁶, Martin Schaier⁴, Nicolas Sgarioto⁸, Noël J.-M. Raynal⁸, Karin Nowikovsky^{6,7}, Wolfgang M. Schmidt¹⁰, Petra Heffeter^{1,3}, Samuel M. Meier-Menches^{2,4,5}, Gunda Koellensperger⁴, Bernhard K. Keppler^{2,3}, Walter Berger^{1,3}*

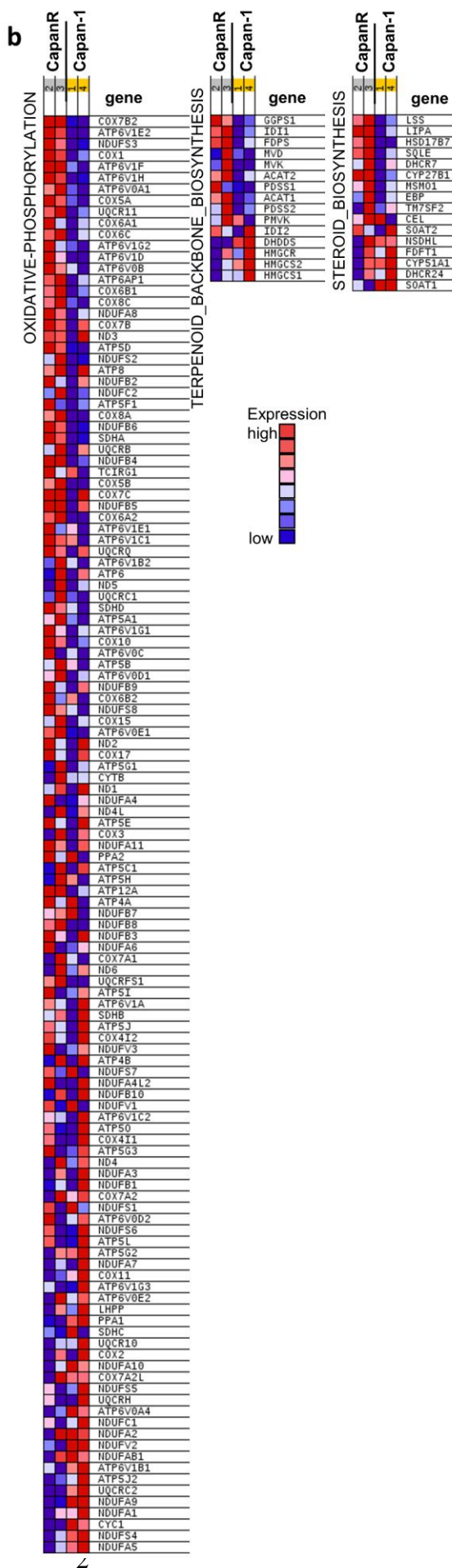
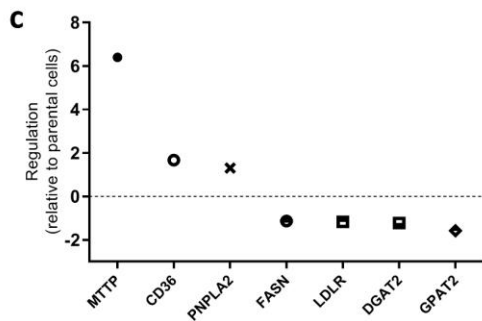
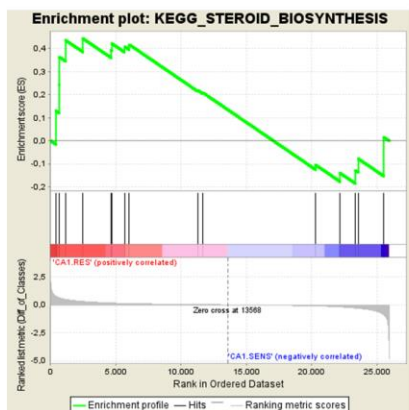
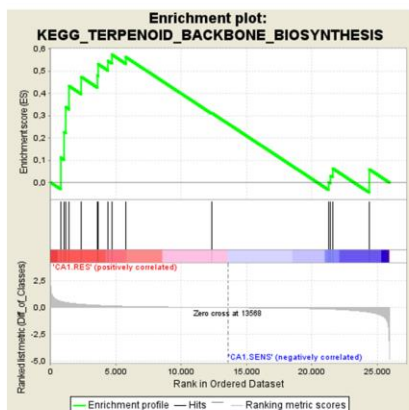
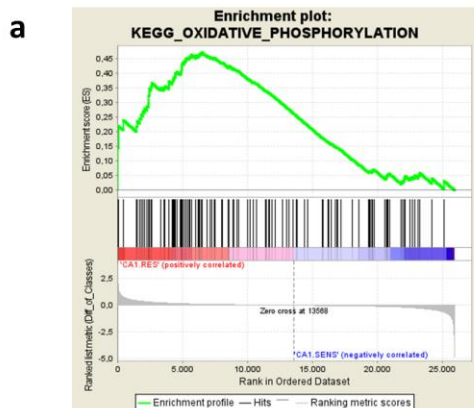


Figure S1. Acquired BOLD-100 resistance of Capan-1 cells is associated with transcriptional deregulation of the lipid metabolism. a) GSEA identifies “OXIDATIVE_PHOSPHORYLATION” (nominal p -value $<E^{-7}$; FDR q -value=0.121) and “TERPENOID_BACKBONE_BIOSYNTHESIS” (nominal p -value=0.169; FDR q -value=0.652) as the third and sixth top enriched gene sets, respectively, from the KEGG database in CapanR vs. Capan-1 cells. b) Heatmaps of respective top enriched gene sets identified from GSEA in CapanR vs. Capan-1 cells. c) Regulation of specific genes involved in fatty acid and cholesterol metabolism of CapanR vs. Capan-1 cells (indicated as dashed line at 0). mRNA levels with a fold change $> |1.1|$ were considered for graphical display.

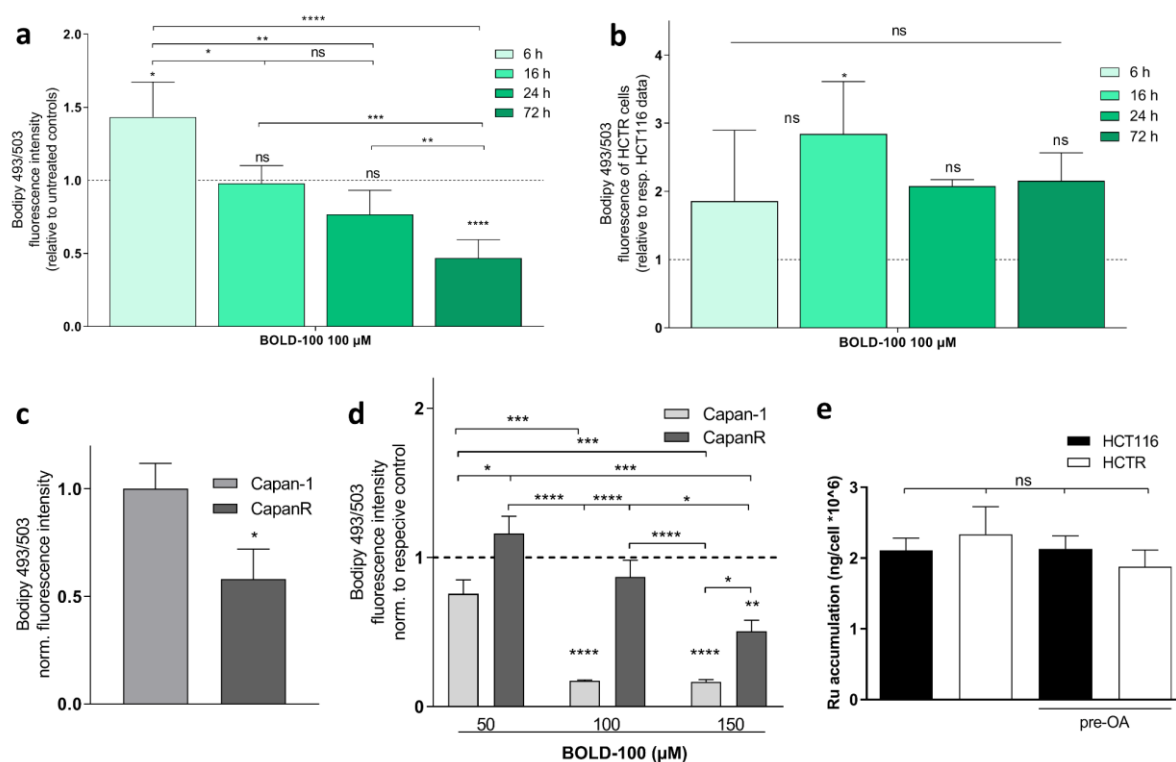


Figure S2. Cellular lipid content is modulated by and affects the anticancer activity of BOLD-100. a) Fluorescence intensity of parental HCT116 cells after treatment with 100 μ M of BOLD-100 for indicated time frames normalized to controls (depicted as dashed line) determined by flow cytometry after staining with 0.5 μ M Bodipy 493/503 for 15 min. One-way ANOVA with Bonferroni's multiple comparisons test: * p <0.05, *** p <0.0001, **** p <0.0001, ns: non-significant. b) Bodipy 493/503 fluorescence intensity of HCTR cells after treatment with 100 μ M of BOLD-100 for indicated time frames normalized to corresponding HCT116 cells (depicted as dashed line) determined by flow cytometry after staining with 0.5 μ M of Bodipy 493/503 for 15 min. One-way ANOVA with Bonferroni's multiple comparisons test: * p <0.05, ns. c) Normalized fluorescence intensity of Capan-1 and CapanR cells determined by FACS after staining with 0.5 μ M of Bodipy 493/503. Unpaired two-tailed student's t-test: * p <0.05. d) Fluorescence intensity of Capan-1 and CapanR cells treated with the indicated concentrations of BOLD-100 for 72 h determined by FACS after staining with 0.5 μ M of Bodipy 493/503 for 15 min. Data are normalized to the respective

controls. Two-way ANOVA with Tukey's multiple comparisons test: $*p<0.05$, $**p<0.005$, $***p<0.0005$, $****p<0.0001$. e) ICP-MS analyses of whole cell lysates of BOLD-100-sensitive and -resistant HCT116 cells after 72 h pre-treatment with 100 μM of OA and 24 h of treatment with 100 μM of BOLD-100. One-way ANOVA with Bonferroni's multiple comparisons test: ns.

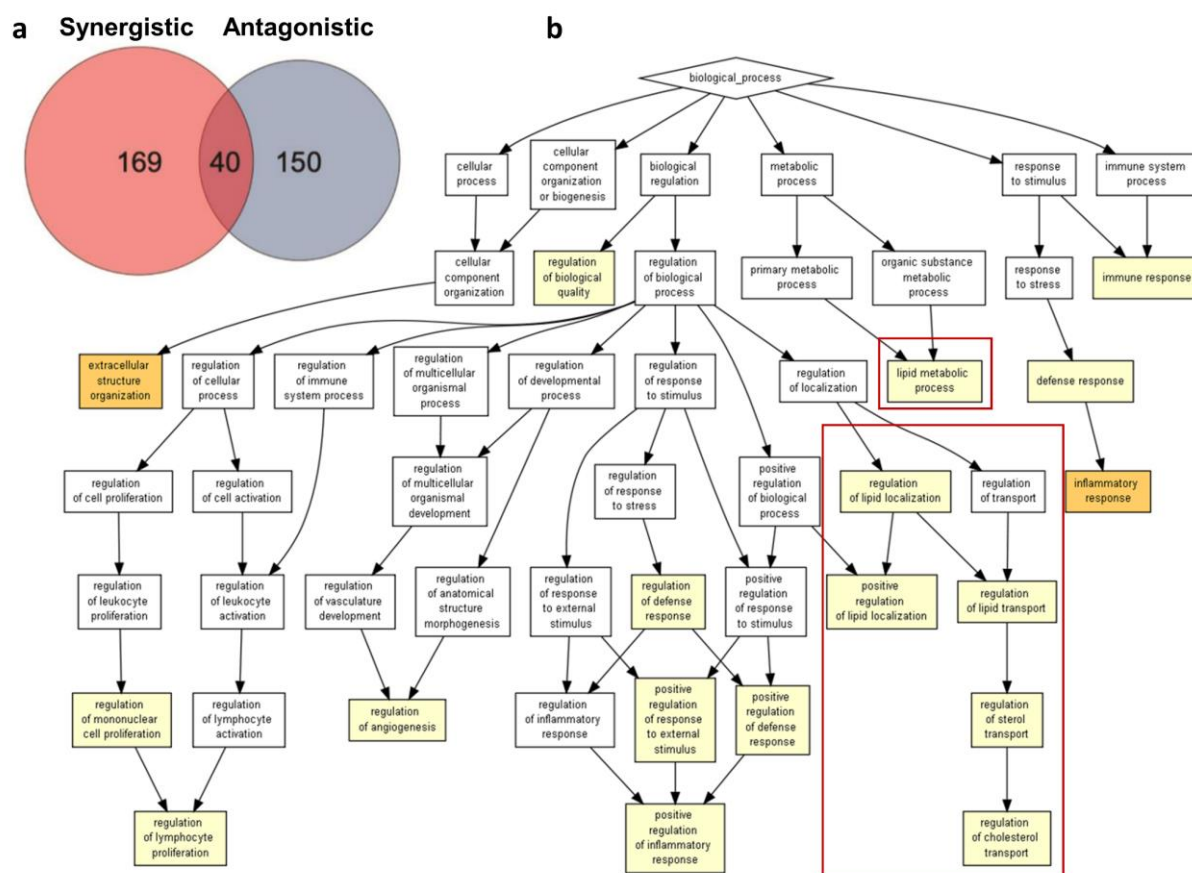


Figure S3. Drugs synergizing with BOLD-100 impact lipid metabolic processes. a) Venn diagram of gene selection process of unbiased drug-gene interaction screens of 1760 compounds where 129 genes were associated with synergistic drugs and 110 genes were associated with antagonistic drugs. b) Biological process analysis of genes associated with synergistic hits. Lipid processing- and regulation of sterol transport associated hits are displayed in red boxes.

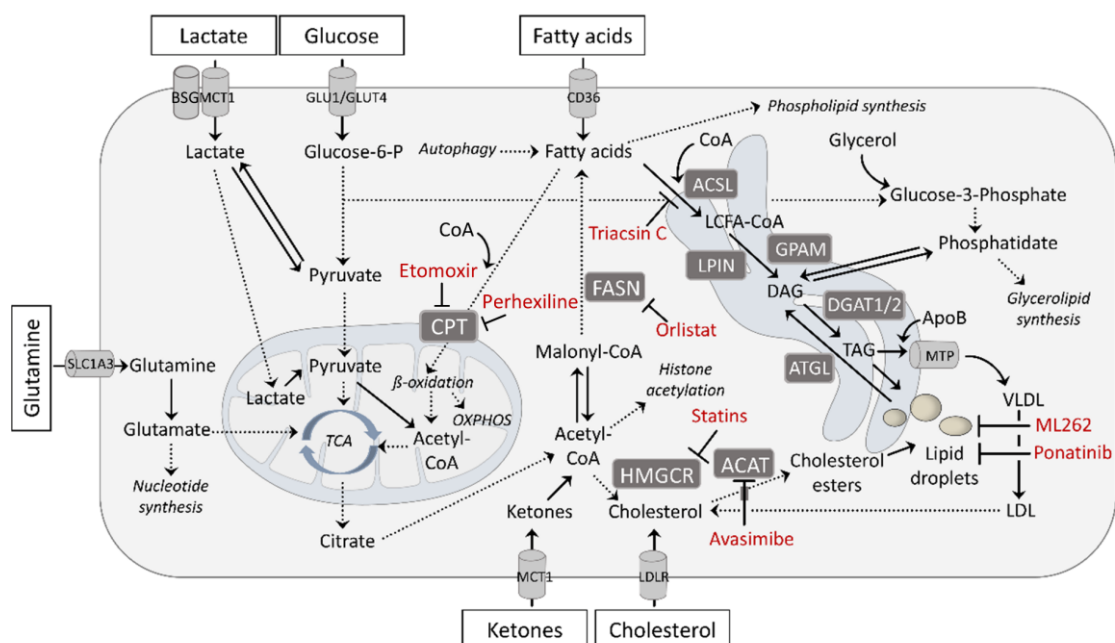


Figure S4. Scheme of drug-respective modes of action. Drugs are indicated in red. Building blocks for schematic representation were provided by © Motifolio (license holder: T. Mohr).

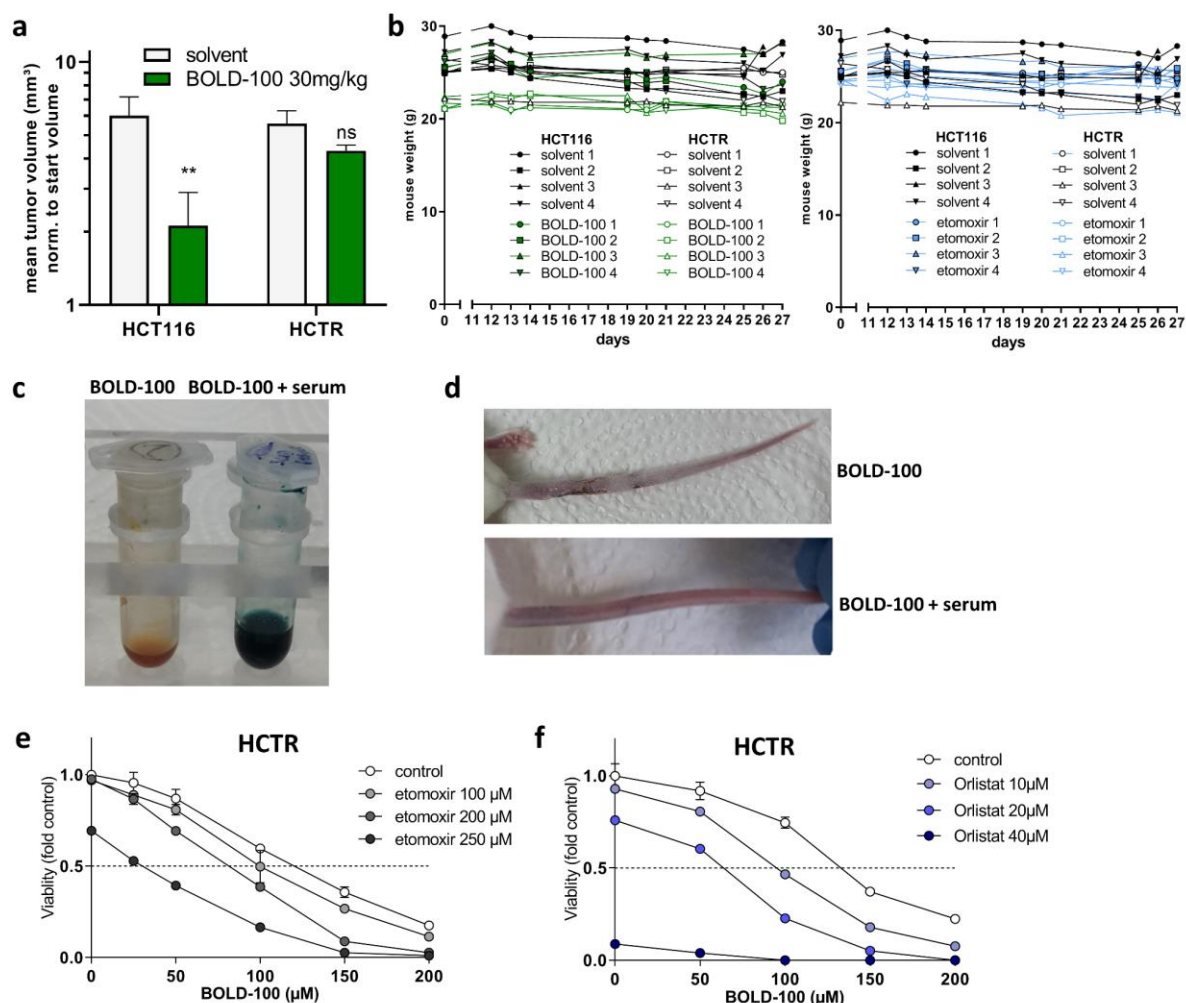


Figure S5. BOLD-100 significantly reduced HCT116, but not HCTR xenograft growth, and did not decrease mouse weight. a) Impact of BOLD-100 on HCT116 or HCTR xenograft growth depicted representatively by the tumor volume at day 27 after inoculation presented as means \pm SEM. Statistical significance was tested by two-way ANOVA with Sidak's multiple comparisons test: $*p < 0.05$; $n = 4$ per experimental group. b) Monitoring of individual mouse weights over 27 days of the course of the in vivo experiment. Left: BOLD-100 compared to solvent control, right graph: etomoxir compared to solvent control. c) BOLD-100 dissolved in 0.9 % NaCl (left, yellow-brownish) as compared to BOLD-100 dissolved in 0.9 % NaCl co-incubated with mouse serum for 2 min (right, green-blueish). d) Tails of mice treated without (upper) or with (lower) serum pre-incubation before treatment. e, f) Cell viability assays after

72 h of treatment with BOLD-100 in combination with e) etomoxir or f) orlistat at indicated concentrations were performed. One representative of three independent experiments is shown.

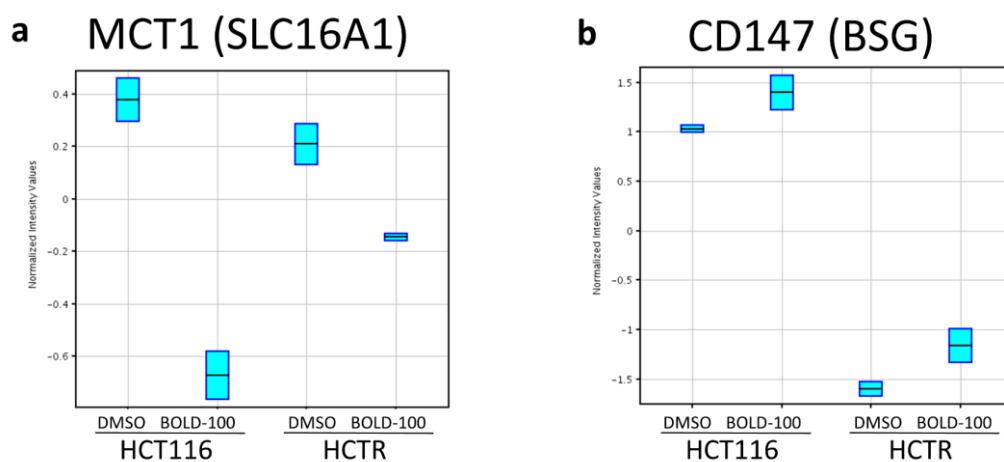


Figure S6. mRNA expression changes of MCT1 and its cofactor CD147 in response to BOLD-100. a) Relative mRNA expression levels of *SLC16A1* and b) *BSG* in HCT116 and HCTR cells after 6 h of treatment with or without 100 μ M of BOLD-100.

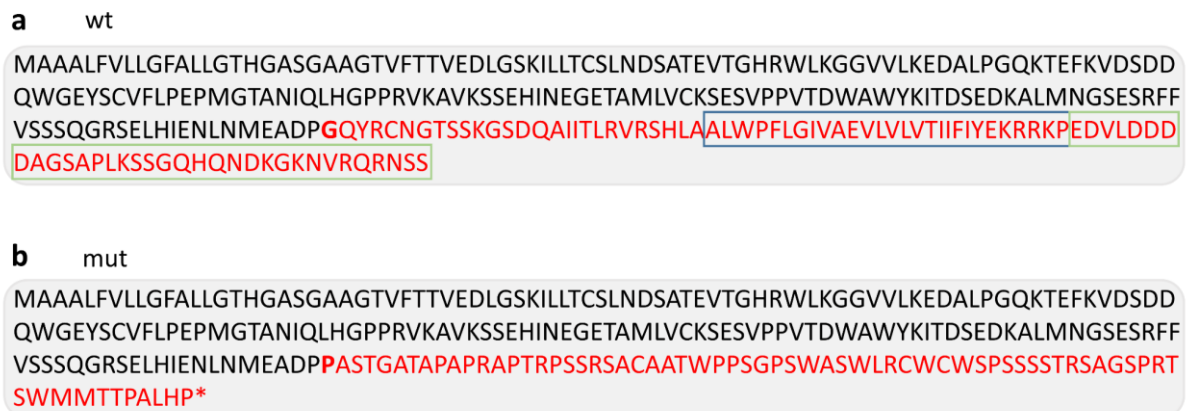


Figure S7. WES reveals frameshift-inducing insertion mutation of *BSG* in HCTR cells. Affected CD147 protein a) reference (wt) vs. b) predicted sequence (mut) of *BSG* NM_198589.3:exon5:c.539_540dup: p.(Gly181Profs*70) in HCTR cells; blue box: TM, green box: cytoplasmic domain of reference wt protein sequence.

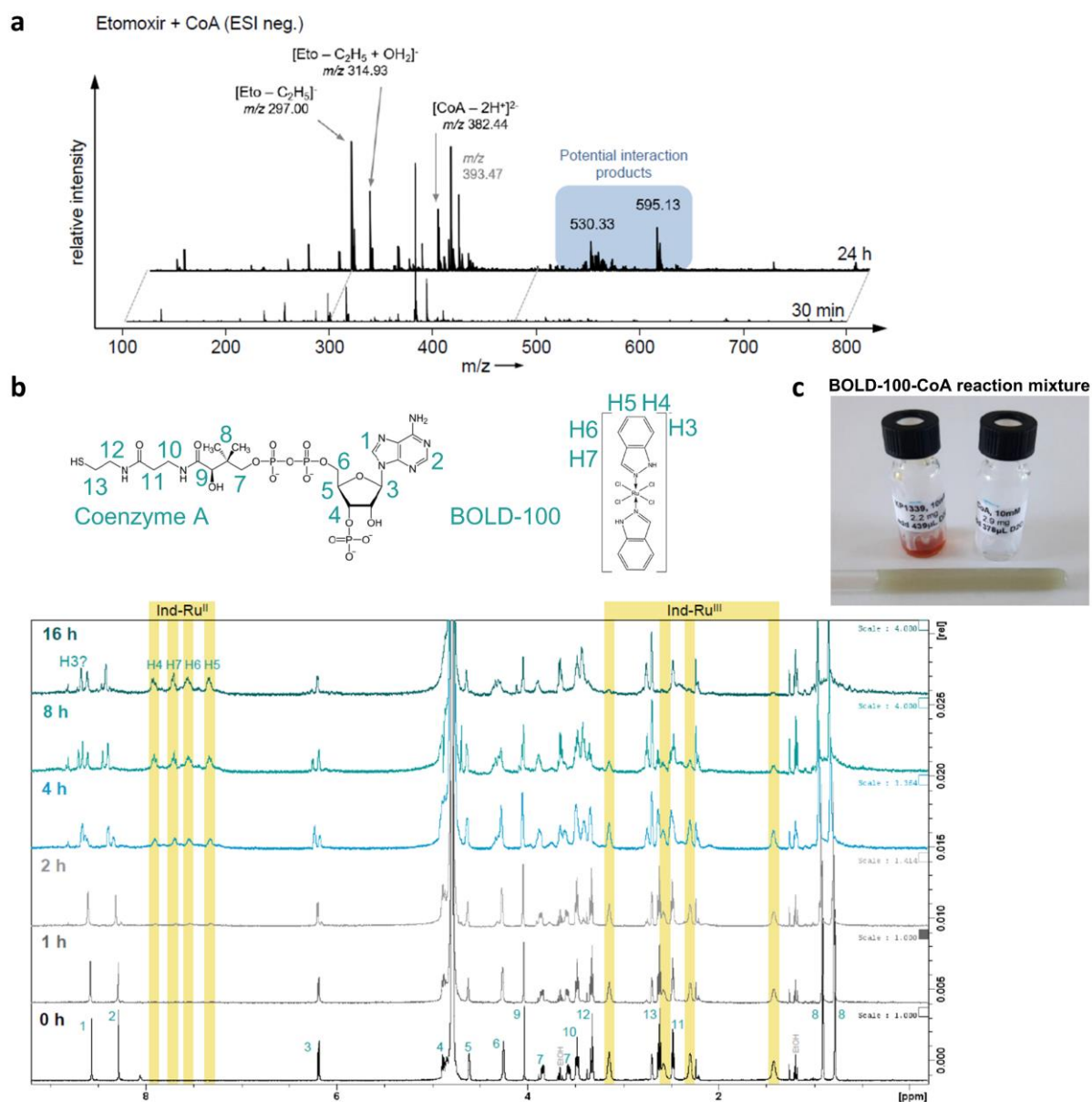


Figure S8. Co-incubation of BOLD-100 with CoA leads to spontaneous adduct formation in a similar mode as etomoxir. a) Mass spectra of the interaction between etomoxir and CoA (1:1 molar ratio) acquired in the negative ion mode after the indicated incubation times. b) ^1H NMR spectra of CoA and BOLD-100 (1:1 molar ratio) acquired over the indicated incubation time. c) Characteristic color shift of the BOLD-100-CoA reaction mixture (reaction tube).

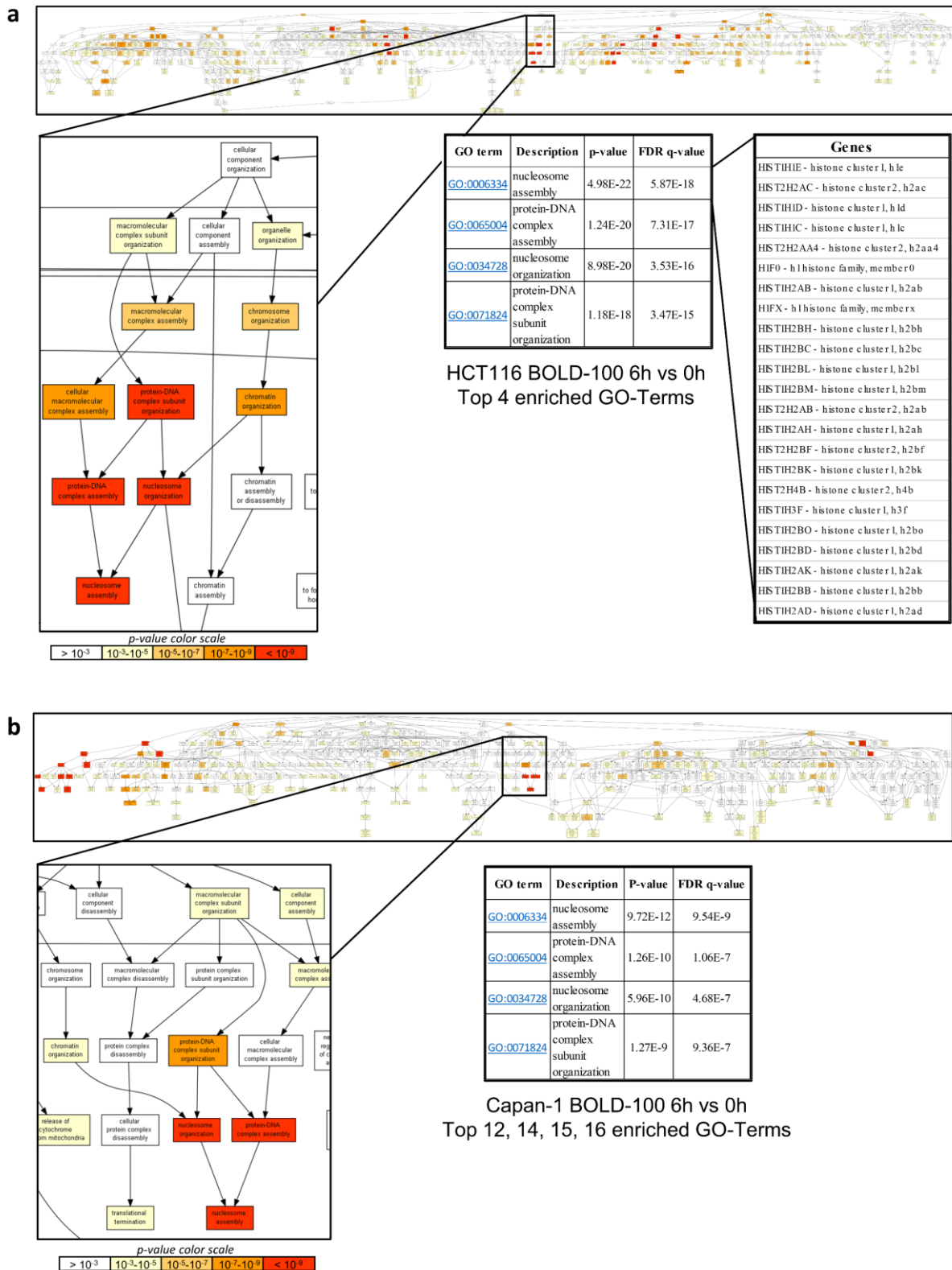


Figure S9. BOLD-100 treatment induces enrichment of GO-terms associated with histone regulation and organization. Enrichment of selected GO-terms after 6 h of treatment with BOLD-100 compared to untreated a) HCT116 or b) Capan-1 cells.

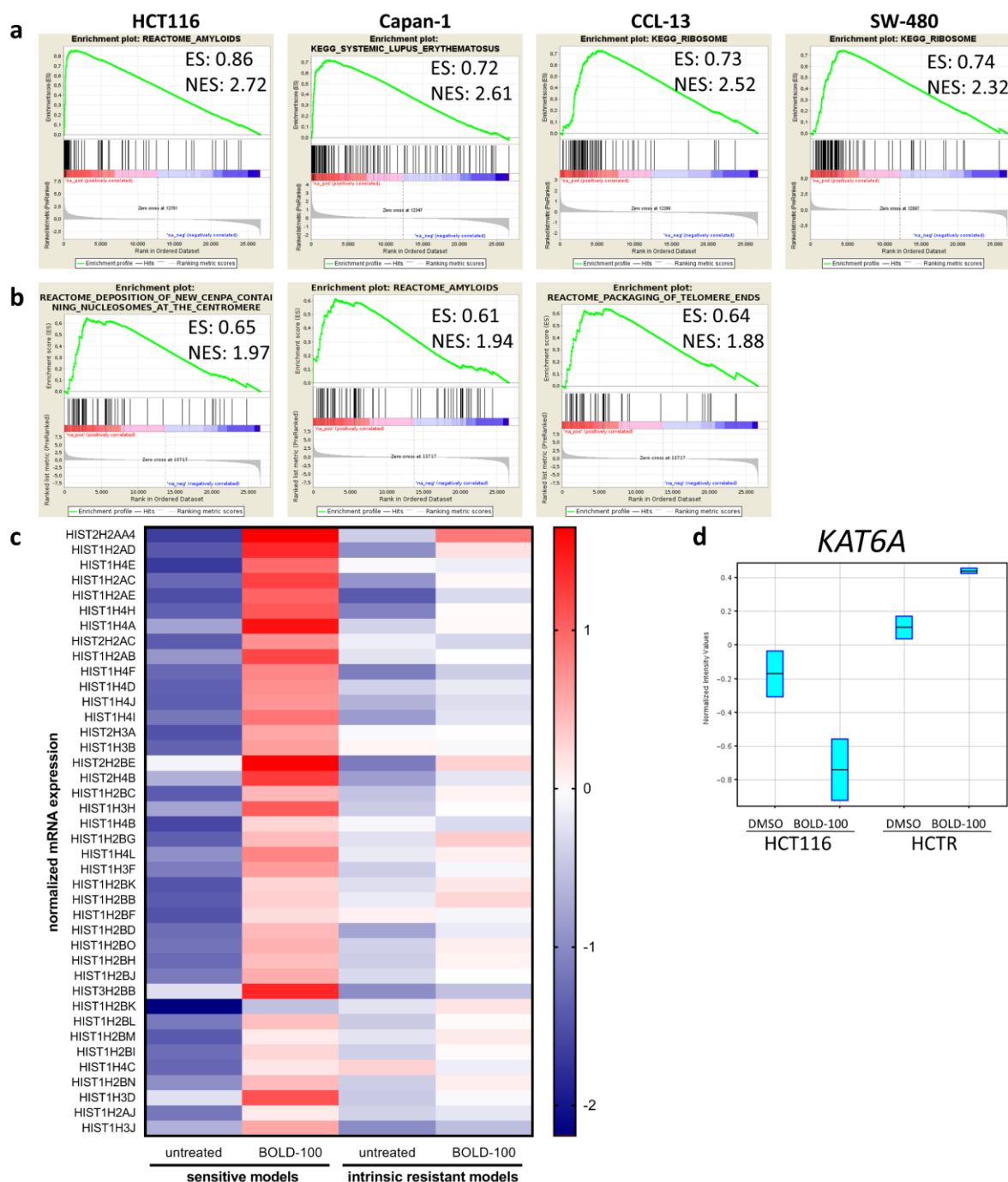


Figure S10. BOLD-100 treatment upregulates histone gene expression of sensitive but not intrinsically resistant cell models. a) GSEA identifies “REACTOME_AMYLOIDS” and “SYSTEMIC_LUPUS_ERYTHEMATOSUS” as top enriched gene sets under 6h BOLD-100 treatment compared to untreated controls in sensitive HCT116 and Capan-1 cells, respectively. In intrinsically resistant CCL-13 and SW480 cells, GSEA identifies “KEGG_RIBOSOME” as

top enriched gene set under BOLD-100 treatment. b) GSEA identifies histone-associated gene sets as top three enriched in untreated pooled intrinsically resistant as compared to pooled sensitive models. c) Heat map displaying normalized mRNA expression of histone genes of the top enriched gene set “REACTOME_AMYLOIDS” in pooled sensitive vs. intrinsically resistant models in response to BOLD-100 vs. untreated control (FC>2). d) Relative mRNA expression levels of *KAT6A* in HCT116 and HCTR cells after 6 h of treatment with or without 100 μ M of BOLD-100.

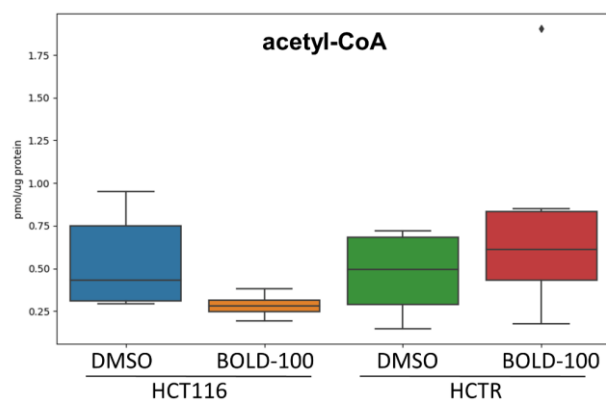


Figure S11. BOLD-100 treatment reduces acetyl-CoA only in parental HCT116 cells. Impact of BOLD-100 (24h, 100 μ M) or solvent control DMSO exposure on the level on acetyl-CoA (pmol/ μ g protein, n=6 biological replicates) in HCT116 and HCTR cells as determined by metabolomics analysis.